Nature Communications

https://doi.org/10.1038/s41467-026-68840-3

Article in Press

Radical defluoroallylation of polyfluoroalkyl compounds with alkenes via synergistic photoredox/cobalt catalysis

Received: 17 April 2025

Accepted: 19 January 2026

Cite this article as: Ren, D., Deng, S., Wang, Y. *et al.* Radical defluoroallylation of polyfluoroalkyl compounds with alkenes via synergistic photoredox/cobalt catalysis. *Nat Commun* (2026). https://doi.org/10.1038/s41467-026-68840-3

Demin Ren, Shuang Deng, Yatao Wang, Wei Ding, Pengjie Wang, Jia Yan, Shengchun Wang, Jiaxin Yuan, Baoquan Wan, Xiaotian Qi, Aiwen Lei & Hong Yi

Radical defluoroallylation of polyfluoroalkyl compounds with alkenes via synergistic photoredox/cobalt catalysis

Authors: Demin Ren[1], Shuang Deng[2], Yatao Wang[1], Wei Ding[1], Pengjie Wang[1], Jia Yan[1], Shengchun Wang[1], Jiaxin Yuan,[3]* Baoquan Wan,[4] Xiaotian Qi[1]*, Aiwen Lei[1,2,3]* and Hong Yi[1]*

Affiliations:

[1]Institute for Advanced Studies (IAS), Wuhan University, Wuhan 430072, P. R. China.

[2] College of Chemistry and Molecular Sciences, Wuhan University, Wuhan 430072, P. R. China.

[3]State Key Laboratory of Power Grid Environmental Protection, College of Chemistry and Molecular Sciences, Wuhan University, Wuhan 430072, P. R. China.

[4]State Key Laboratory of Power Grid Environmental Protection, China Electric Power Research Institute, Wuhan 430074, Hubei, China

*Corresponding author. Email: yjx98571@163.com; qi7xiaotian@whu.edu.cn; aiwenlei@whu.edu.cn; hong.yi@whu.edu.cn

Abstract: Selective functionalization and high-value conversion of polyfluoroalkyl compounds is of paramount importance due to their widespread use in pharmaceuticals, agrochemicals, and advanced materials. However, the formidable stability of C(sp^3)–F bonds, exacerbated by strong electron-withdrawing effects, steric hindrance, and the inherent challenge of achieving precise selectivity, has significantly hampered efforts toward their controlled activation and modification. Herein, we present a dual photoredox/cobalt catalytic strategy that enables redox-driven defluoroallylation of perfluoroalkylarenes and polyfluorinated aliphatic amides. Our approach leverages single-electron reduction to cleave robust C(sp^3)–F bonds, generating reactive perfluoroalkyl radicals that couple efficiently with simple alkenes. Cobalt-mediated hydrogen atom transfer, with Lewis acidic fluorine scavengers serving primarily to trap the fluoride and suppress back-electron transfer, ensures precise regioselective allylation under mild conditions. Mechanistic investigations reveal that controlled radical generation and selective activation underpin the unique site selectivity observed. This dual catalytic platform offers an efficient strategy for the construction of complex fluorinated scaffolds and expands the toolkit for the selective transformation of polyfluorinated frameworks.

Introduction:

Polyfluoroalkyl substituents impart unique physicochemical properties—high thermal and chemical stability, hydrophobicity, and distinctive interfacial behavior—that underpin their broad applications in pharmaceuticals, agrochemicals, and advanced materials[1-4]. These features originate from the exceptional strength and polarity of C(sp^3)–F bonds, which simultaneously confer robustness and impede selective activation. The high bond dissociation energies and strong electron-withdrawing effects of these bonds frequently lead to unselective pathways and competing multi-bond cleavage[5-8], underscoring the continued need for catalytic strategies capable of controlling C–F functionalization with precision.

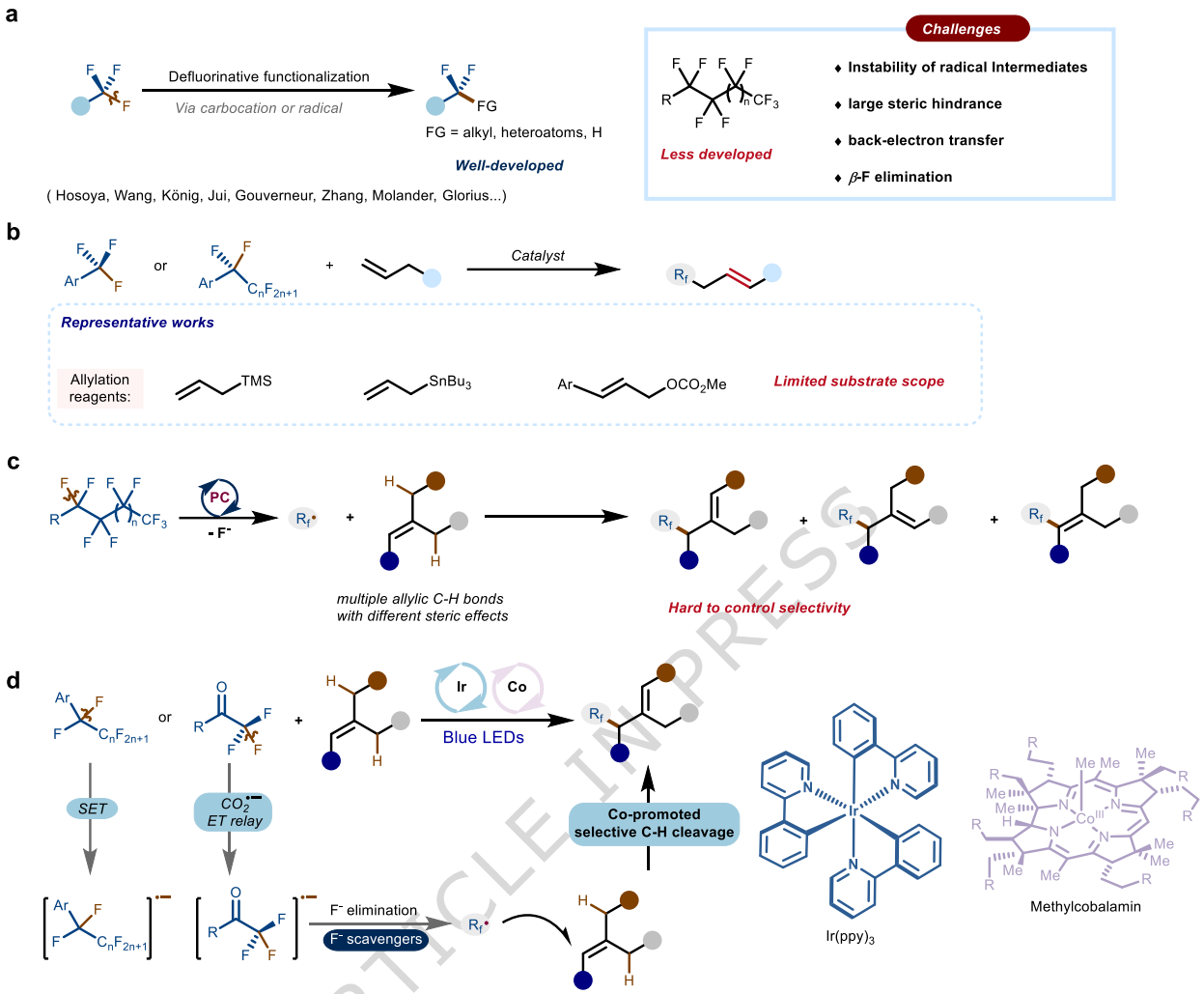

Fig. 1 Challenges in C(sp^3)–F activation of polyfluoroalkyl groups and our defluoroallylation strategy. a) Recent advances in C(sp^3)–F activation and challenges in activating longer perfluoroalkyl groups. **b)** Limitations of prefunctionalized reagents in catalytic defluoroallylation **c)** Site-selectivity challenge in defluoroallylation of alkenes with multiple similar allylic C–H bonds. Color-coded spheres indicate distinct allylic C–H sites with comparable electronic and steric environments. **d)** This work: synergistic photoredox/cobalt catalysis enables radical defluoroallylation of polyfluoroalkyl compounds with alkenes.

Considerable attention has been devoted to the selective activation of trifluoromethyl groups and their derivatives[9-13], and Lewis acid-promoted difluorocarbocation formation[14-16], radical spin–center shifts[17], and photoredox-mediated single-electron processes[18-24] have enabled diverse C–F transformations of CF_3-containing substrates. In contrast, the selective functionalization of longer perfluoroalkyl chains (C_nF_{2n+1}, $n \geq 2$) remains far less developed. Representative examples include the electroreductive α-C–F cleavage of pentafluoroethylarenes followed by CO_2 carboxylation[25], Mg/TMSCl- or Cu–Mg-mediated reductive activation, which predominantly affords silylated or reduced products with limited control over site selectivity[26], and Ni(0)-enabled sequential double C–F activation of pentafluoroethyl alkenes in [3+2] cycloadditions with alkynes[27]. Photoredox-mediated benzylic defluoroallylation of Ar–^{n}C$_4$F$_9$, Ar–^{n}C$_6$F$_{13}$, and Ar–CF(CF$_3$)$_2$ scaffolds has also been demonstrated using allylic stannanes as coupling partners[28], while sequential organophotocatalytic/Lewis acidic protocols enable benzylic C–F substitution with carbon nucleophiles such as allylsilanes, stannanes, and silyl enol ethers[29]. Although these studies demonstrate that longer perfluoroalkyl groups can undergo C–F activation under tailored

conditions, they uniformly rely on prefunctionalized coupling partners and often require strongly reducing or Lewis acidic media, and none provides a general method for direct C–C bond formation with simple, unfunctionalized alkenes. Beyond these methodological constraints, the strong electron-withdrawing nature of perfluoroalkyl groups destabilizes the radical intermediates formed upon C–F cleavage, making them highly susceptible to competing pathways. These challenges—including steric hindrance, radical destabilization, and reverse processes such as back electron transfer (BET) and fluoride readdition—often suppress productive reactivity[30-34](Fig. 1a). These intrinsic features complicate the selective incorporation of perfluoroalkyl motifs into pharmacophores and complex molecular scaffolds, underscoring the need for broadly applicable catalytic strategies.

Alkenes are privileged building blocks in synthesis, offering diverse modes of reactivity for the rapid construction and late-stage modification of complex molecules[35-36]. In particular, allylic C–H functionalization has attracted significant attention for its ability to introduce multifunctional motifs while preserving the integrity of the olefinic bond[37-40]. Despite advances in catalytic defluoroallylation, current methodologies predominantly rely on prefunctionalized reagents such as allylsilanes or allylstannanes[11,16,28,41], which exhibit limited substrate scope (Fig. 1b). A more streamlined strategy would enable the direct defluoroallylation of simple alkenes using perfluoroalkyl compounds without prefunctionalization. Such a transformation would be especially valuable in complex settings—such as natural products bearing multiple, electronically and sterically similar allylic C–H sites—where achieving high levels of site selectivity remains difficult (Fig. 1c).

To surmount the challenge of direct C(sp^3)–F activation in perfluoroalkylarenes and their subsequent coupling with alkenes, we propose a synergistic radical strategy that combines photoredox and cobalt catalysis (Fig. 1d). We hypothesize that a photoredox catalyst can reduce perfluoroalkyl compounds to generate unstable radical anions, which then eliminate fluoride to give perfluoroalkyl radicals. Steric hindrance may further impede bond formation, potentially leading to reversibility via back electron transfer or fluoride readdition. To address these issues, we introduce Lewis acidic fluorine scavengers to accelerate radical generation and suppress undesired electron transfer[42-43], thereby enhancing overall reaction efficiency. The perfluoroalkyl radicals thus formed are expected to add smoothly to alkenes, with subsequent cobalt-catalyzed hydrogen atom transfer[44-46] (HAT) facilitating the regioselective formation of the desired products. In this work, we demonstrate a dual photoredox/cobalt catalytic system that enables redox-driven, site-selective allylation of perfluoroalkylarenes and polyfluorinated aliphatic amides. This methodology provides an efficient and complementary strategy for the selective transformation of perfluoroalkyl and polyfluorinated compounds, enabling the precise assembly of complex molecular scaffolds.

Results

In our initial investigations, we selected methyl 4-(perfluorobutyl)benzoate (**1a**) and 2-methylpent-1-ene (**2af**) as model substrates. Systematic optimization (Table 1) established the optimal conditions (Condition A): 0.5 mol% *fac*-Ir(ppy)$_3$ as the photocatalyst, 3 mol% methylcobalamin as the HAT catalyst, 0.25 equivalents of DIPEA, and 0.3 equivalents of HBpin, which functions as both base and fluoride scavenger. Reactions conducted in 2-ethoxyethanol under blue LED irradiation for 36 hours afforded the desired product **3af** in 85% yield by GC analysis (83% isolated yield, Table 1, entry 1). Replacing *fac*-Ir(ppy)$_3$ with [Ir(dtbbpy)(ppy)$_2$]PF_6, Ir[FCF_3(CF_3)ppy]$_2$(4,4'-dCF_3bpy)PF_6, or Mes-$Acr^+BF_4^-$ resulted in only trace or no product

(entries 2–4). Similarly, methylcobalamin proved essential for high yield and exclusive site selectivity, as alternative cobalt catalysts (B_{12}, Co-TPP, CoPc, or cobaloxime complexes) significantly reduced the reaction outcome (entries 5–10). Reducing the equivalents of olefin **2af** decreased the yield to 77% (entry 11), while substituting DIPEA with K_2CO_3 or 2-ethoxyethanol with DMSO led to diminished yields of 68% and 32%, respectively (entries 12–13). Moreover, alternative boron reagents (B_2pin_2, Et_3B) provided unsatisfactory results (entries 14–15). Control experiments showed that $Ir(ppy)_3$, methylcobalamin, and visible light are essential for the reaction (entries 16–18), while DIPEA and HBpin improve the reaction efficiency (entries 19–20).

Table 1 | Reaction optimization

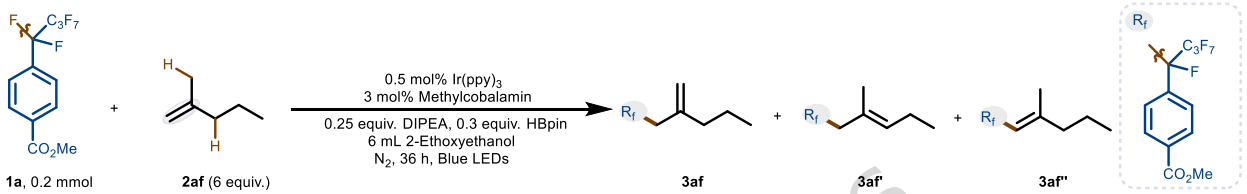

Entry	Variation from the standard conditions	Yield of **3af**	Ratio of **3af** : Others
1	none	85% (83%)[a]	> 20 : 1
2	$[Ir(dtbbpy)(ppy)_2]PF_6$ instead of $Ir(ppy)_3$	Trace	-
3	$Ir[FCF_3(CF_3)ppy]_2(4,4'\text{-}dCF_3bpy)PF_6$ instead of $Ir(ppy)_3$	N.d.	-
4	$Mes^-Acr\ BF_4^-$ instead of $Ir(ppy)_3$	N.d.	-
5	B_{12} instead of Co-1	71%	> 20 : 1
6	Co-2 instead of Co-1	64%	87 : 13
7	Co-3 instead of Co-1	17%	74 : 26
8	Co-4 instead of Co-1	24%	65 : 35
9	Co-5 instead of Co-1	21%	81 : 19
10	Co-6 instead of Co-1	53%	72 : 28
11	4 equiv. **2a** was used	68%	> 20 : 1
12	K_2CO_3 instead of DIPEA	68%	> 20 : 1
13	DMSO instead of 2-Ethoxyethanol	32%	> 20 : 1
14	B_2pin_2 instead of HBpin	77%	> 20 : 1
15	Et_3B instead of HBpin	74%	> 20 : 1
16	*w/o* light	N.d.	-
17	*w/o* $Ir(ppy)_3$	N.d.	-
18	*w/o* Methylcobalamin	12%	75 : 25
19	*w/o* DIPEA	61%	95 : 5
20	*w/o* HBpin	63%	> 20 : 1

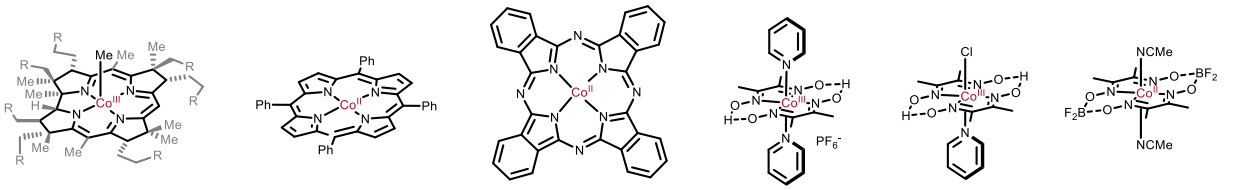

Reaction condition: a solution of (methyl 4-(perfluorobutyl)benzoate **1a** (70.8 mg, 0.2 mmol), 2-methylpent-1-ene **2af** (100.8 mg, 6.0 equiv.), *fac*-Ir(ppy)$_3$ (0.5 mol%, 0.65 mg), cobalt catalyst (3 mol%), boron reagents (0.3 equiv.) and base (0.25 equiv.) in degassed 2-ethoxyethanol (6.0 mL) were stirred under nitrogen atmosphere and irradiated by 3W blue LEDs for 36 h. All yields based on gas chromatography (GC) analysis with *n*-pentadecane as an internal standard. All regioselectivities were determined by GC and NMR. N.d.: Not detected. [a]Isolated yield.

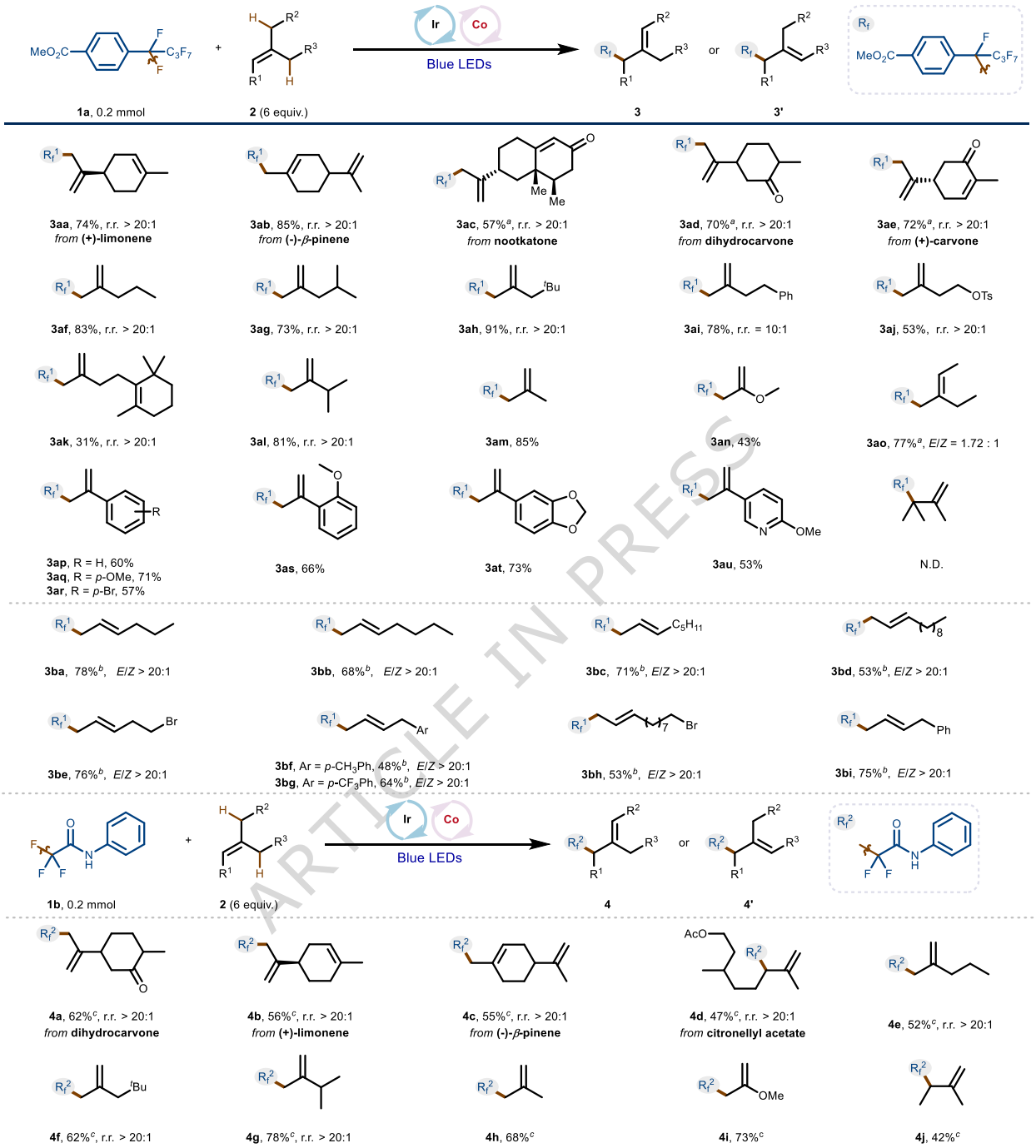

Fig. 2 | Scope of alkene substrates. Reaction conditions: **1a** (0.2 mmol), **2** (6 equiv.), *fac*-Ir(ppy)$_3$ (0.5 mol%), methylcobalamin (3 mol%), HBpin (0.3 equiv.) and DIPEA (0.25 equiv.) in degassed 6 mL 2-ethoxyethanol, blue LEDs, 36 h, under nitrogen. [a]**1a** (0.2 mmol), alkene **2** (6 equiv.), *fac*-Ir(ppy)$_3$ (1 mol%), methylcobalamin (3 mol%), DIPEA (0.5 equiv.), NaOAc (0.5 equiv.), LiF (0.5 equiv.) in degassed 6 mL 2-ethoxyethanol, blue LEDs, 48 h, under nitrogen. [b]**1a** (0.2 mmol), **2** (6 equiv.), *fac*-Ir(ppy)$_3$ (1 mol%), Co-TPP (3 mol%), HBpin (0.3 equiv.) and DIPEA (0.25 equiv.) in degassed 6 mL 2-ethoxyethanol, blue LEDs, 48 h, under nitrogen. [c]**1b** (0.2 mmol), **2** (6 equiv.), *fac*-Ir(ppy)$_3$ (3 mol%), methylcobalamin (3 mol%), Cs_2CO_3 (1 equiv.) HBpin (1.2 equiv.) and DIPEA (3 equiv.) in degassed 6 mL DMF, 1 atm CO_2 (headspace volume: 14 mL), blue LEDs, 36 h. All yields are isolated yields. All regioselectivity > 20:1.

With the optimized conditions established, we next explored the alkene substrate scope with a particular focus on site selectivity. As summarized in Fig. 2, the reactivity of various natural terpenes, such as (+)-limonene, *β*-pinene, nootkatone, dihydrocarvone, and (+)-carvone (**3aa–3ae**), was explored. These substrates exhibited excellent site selectivity (>20:1), underscoring the efficiency and practicality of our method for modifying complex natural molecules. We subsequently evaluated 1,1-disubstituted alkenes bearing methyl and primary alkyl substituents (**3af–3ak**). Under the optimized conditions, our strategy effectively differentiated between primary and secondary allylic C–H bonds, selectively cleaving the primary site to furnish the desired products exclusively. For 1,1-disubstituted alkenes containing both methyl and secondary alkyl groups (**3al**), the reaction predominantly proceeded via cleavage of the methyl C–H bond, affording the corresponding products. Additionally, a diverse array of disubstituted olefins—including simple alkyl, aryl, and heteroaromatic alkenes incorporating pyridine or benzodioxole motifs (**3am–3au**)—served effectively as fluoroalkyl radical acceptors, delivering the target products in moderate yields. In all cases, selective activation was confined to a single C–F bond; however, tetrasubstituted alkenes failed to react due to steric encumbrance, while monosubstituted alkenes exhibited low conversion and poor selectivity.

To overcome the limitations encountered with monosubstituted alkenes, we optimized the reaction parameters (see Supplementary Table 4). By substituting methylcobalamin with Co-TPP, we achieved effective allylic fluoroalkylation of monosubstituted alkenes (**3ba–3bi**), exhibiting both exceptional site-selectivity and remarkable stereoselectivity (*E*/*Z* > 20:1). Our catalytic system also accommodates trifluoroacetamide substrates; employing $Ir(ppy)_3$ to reduce CO_2 generates the key intermediate $CO_2^{\bullet-}$, which in turn facilitates the selective defluoroalkylation of trifluoroacetamides with excellent chemoselectivity and regioselectivity (**4a–4j**). Furthermore, trisubstituted alkenes—whether simple or derived from natural terpenes—were well tolerated, affording the desired products in moderate to good yields. Collectively, these findings underscore the versatility and robustness of our method, establishing a valuable platform for the selective conversion of diverse olefin substrates into complex fluorinated architectures.

The scope of perfluoroalkyl arenes and trifluoroacetamides was further examined using 2,3-dimethylbut-1-ene (**2al**) under the standard conditions (Fig. 3). In addition to the C_4F_9 group, perfluoroalkyl moieties including C_3F_7, C_6F_{13}, C_8F_{17}, and $C_{10}F_{21}$ underwent selective allylic functionalization via benzylic $C(sp^3)$–F bond cleavage (**5a–5d**). Furthermore, arenes bearing additional electron-withdrawing groups, such as cyano and alkynyl substituents, participated effectively in the reaction (**5e–5f**). *N*-Aryl trifluoroacetamides featuring a diverse range of functional groups were converted selectively to the corresponding products with high chemoselectivity (**5g**–**5l**). For instance, substituents such as methyl, methoxy, 3-fluoro, and 4-chloro were well tolerated, with selective reduction occurring exclusively at the C–F bonds adjacent to the carbonyl group, while the CF_3 moiety remained intact (**5j**), suggesting that C–F bond cleavage is facilitated by the proximal carbonyl. In addition, sensitive functionalities such as alkynes were compatible under the reaction conditions (**5n**), whereas tertiary amides (**5o**–**5q**) exhibited only trace reactivity (<5%). Next, the scope of biologically derived molecules was examined under the standard conditions. Derivatives of D-allofuranose, citronellol, D-menthol, pregnenolone, and cholesterol (**5r**–**5v**) underwent the defluoroallylation, affording the corresponding products in moderate to good yields.

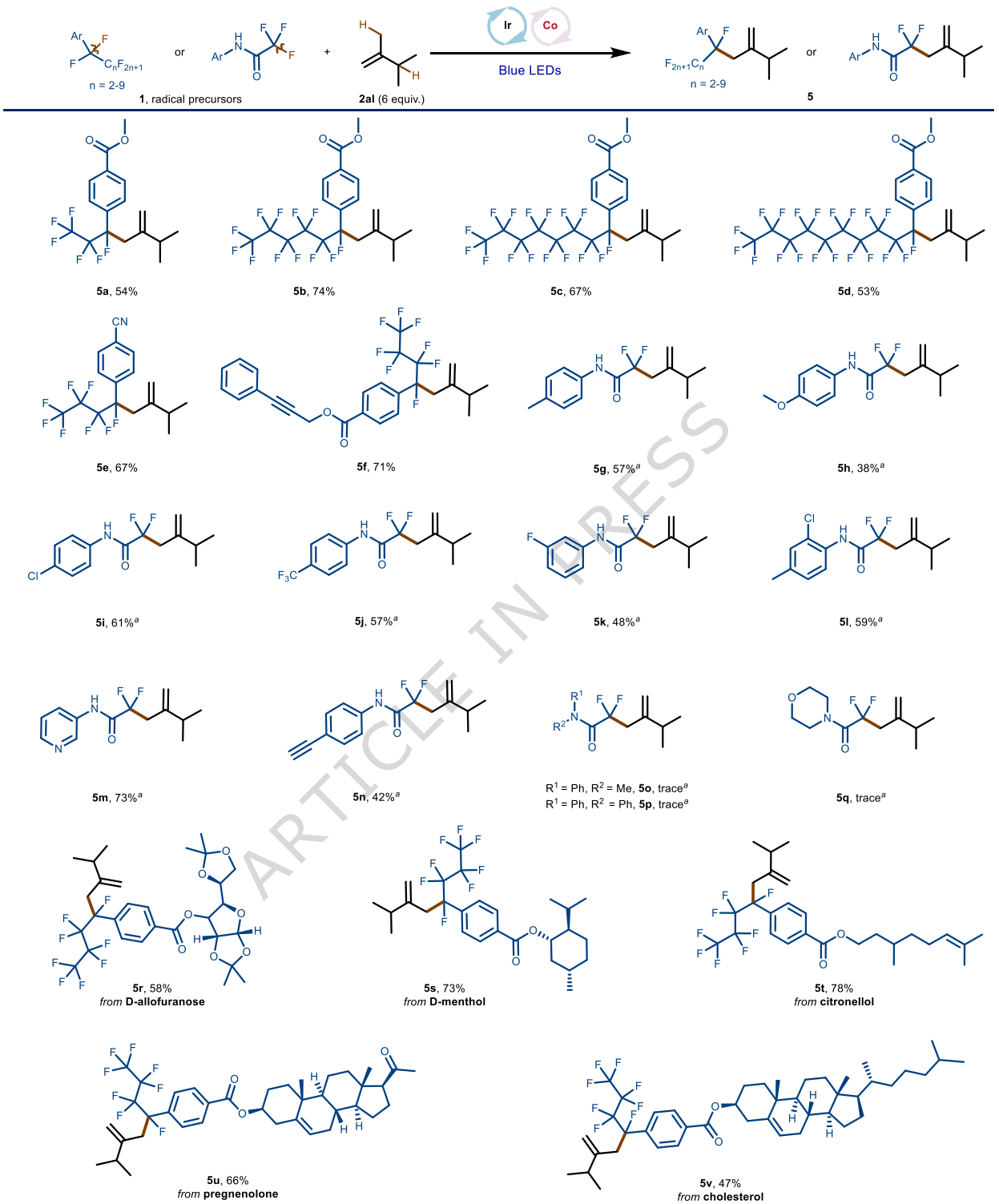

Fig. 3 | Scope of perfluoroalkylarenes and polyfluorinated aliphatic amides for allylic fluoroalkylation. Reaction conditions: **1** (0.2 mmol), **2** (6 equiv.), *fac*-Ir(ppy)$_3$ (0.5 mol%), methylcobalamin (3 mol%), HBpin (0.3 equiv.) and DIPEA (0.25 equiv.) in degassed 6 mL 2-ethoxyethanol, blue LEDs, 36 h, under nitrogen. [a]**1** (0.2 mmol), **2** (6 equiv.), *fac*-Ir(ppy)$_3$ (3 mol%), methylcobalamin (3 mol%), Cs_2CO_3 (1 equiv.) HBpin (2 equiv.) and DIPEA (3 equiv.) in degassed 6 mL DMF, 1 atm CO_2 (headspace volume: 14 mL), blue LEDs, 36 h. All yields are isolated yields. All regioselectivity > 20:1.

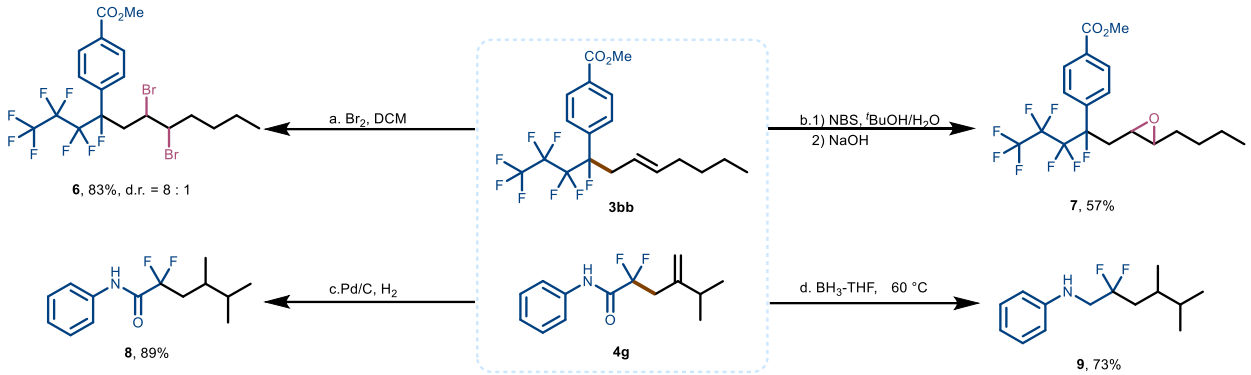

Fig. 4 | Synthetic applications. a) Bromination of **3bb** with Br_2 in DCM. **b)** NBS-mediated oxidative functionalization of **3bb** in $^tBuOH/H_2O$ followed by NaOH. **c)** Hydrogenation of **4g** over Pd/C under H_2. **d)** Reduction of **4g** with BH_3–THF.

To further demonstrate the synthetic utility of this methodology, representative products **3bb** and **4g** were subjected to downstream transformations (Fig. 4). Bromination of **3bb** with Br_2 afforded dibromide **6**, while epoxidation of **3bb** yielded the corresponding epoxide **7**. Catalytic hydrogenation of **4g** with Pd/C gave product **8**. In addition, treatment of **4g** with a BH_3–THF complex reduced both the carbonyl group and the C=C bond, affording *β*-fluoroamine **9**.

To gain more insights into the reaction mechanism, we conducted a series of mechanistic experiments (Figs. 5a–e). Radical trapping experiments revealed that the addition of 2 equivalents of either TEMPO or BHT significantly suppressed the transformation, and HR-MS analysis confirmed the formation of the corresponding fluoroalkyl adducts, supporting a radical pathway (Fig. 5a and Supplementary Figs 1–3). Furthermore, radical-clock experiments employing (–)-*β*-pinene with both substrate classes (methyl 4-(perfluorobutyl)benzoate **1a** and 2,2,2-trifluoro-*N*-phenylacetamide **1b**), afforded the corresponding ring-opened adducts in 85% and 55% yield, respectively, under the standard conditions, further corroborating the involvement of fluoroalkyl radicals (Supplementary Figs. 4–5). Monitoring of the reaction revealed the formation of formate, supporting the involvement of the $CO_2^{\bullet-}$ intermediate generated via single-electron reduction of CO_2[47] (Fig. 5b and Supplementary Figs. 6–9). EPR spectroscopy further confirmed this hypothesis by directly detecting the characteristic signal of $CO_2^{\bullet-}$ under photocatalytic conditions containing only *fac*-Ir(ppy)$_3$ and CO_2, thus providing unequivocal evidence for the single-electron reduction of CO_2 (Fig. 5c and Supplementary Fig. 10). Stern–Volmer luminescence quenching studies revealed that the excited state of *fac*-Ir(ppy)$_3$ was quenched by perfluoroalkylarene **1a**, whereas **2al** and DIPEA exhibited only minor effects. These results support that the photocatalytic cycle is initiated by single-electron transfer (SET) from the excited photocatalyst to **1a**. (Fig. 5d and Supplementary Figs. 11–14).

In the trifluoroacetamide system, neither 2,2,2-trifluoro-*N*-phenylacetamide **1b**, **2al**, nor DIPEA quenched the excited state of *fac*-Ir(ppy)$_3$ (Supplementary Figs. 15–17). These observations collectively suggest that the photocatalytic cycle in this system is not initiated by SET from the excited photocatalyst to the amide substrate. Instead, based on the EPR evidence for $CO_2^{\bullet-}$ formation under conditions containing only *fac*-Ir(ppy)$_3$ and CO_2, it is proposed that the excited photocatalyst transfers an electron to CO_2, generating the $CO_2^{\bullet-}$ intermediate that subsequently engages in the catalytic cycle. Finally, time- course ^{11}B and ^{19}F NMR analyses revealed the progressive emergence of a ^{11}B triplet at $\delta = +5.7$ ppm, accompanied by a ^{19}F multiplet at $\delta \approx -140$ ppm, corresponding to the literature-reported signals for the $[BF_2(pin)]^-$ anion[48,49].

These resonances were absent in the absence of HBpin, indicating that HBpin functions as a fluoride scavenger in the reaction (Fig. 5e and Supplementary Figs. 18–21).

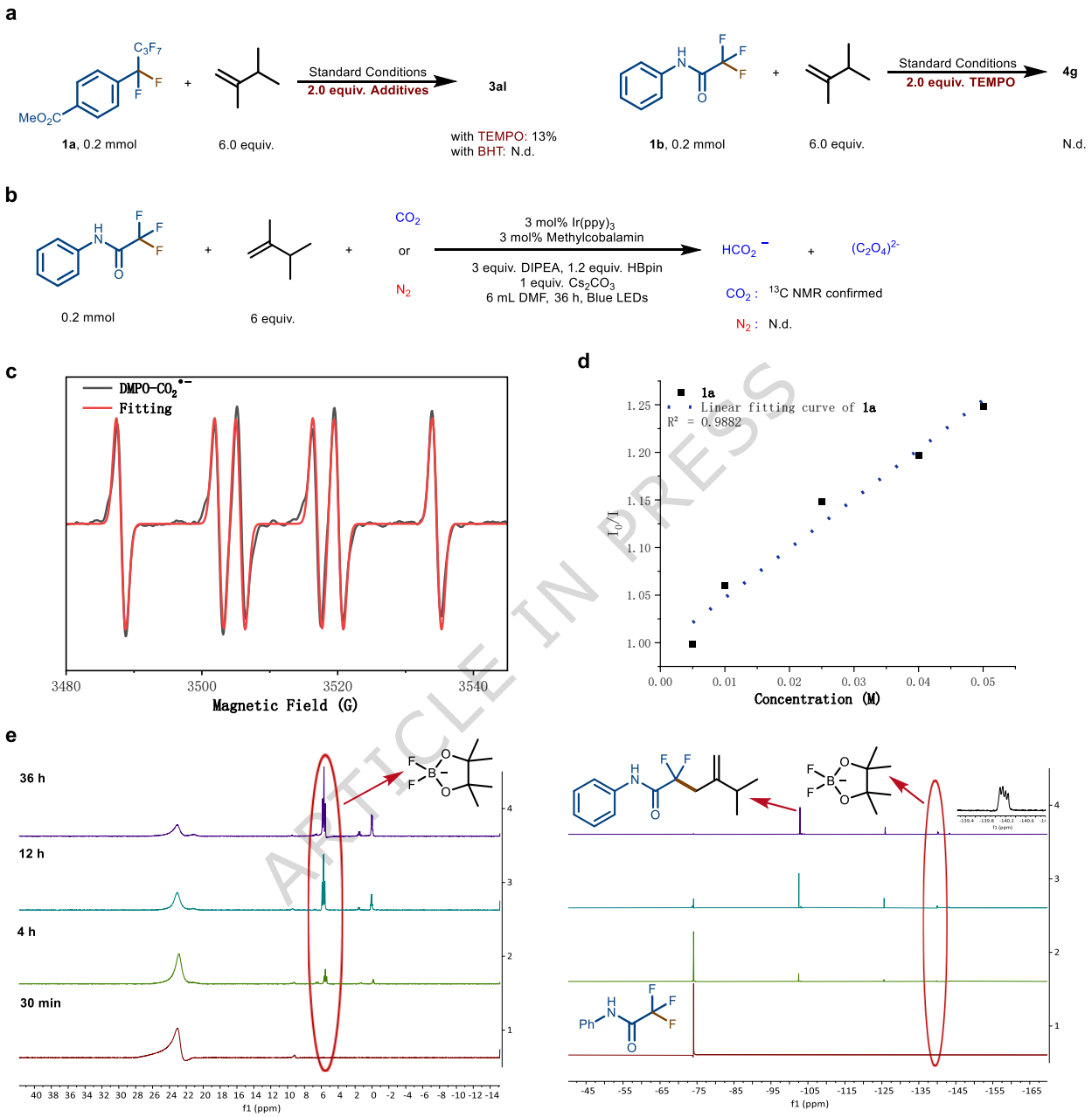

Fig. 5| Mechanistic studies. a) Radical inhibition experiments. N.d.: Not detected. **b)** Detection of HCO^{2-} and $(C_2O_4)^{2-}$ formation. **c)** EPR spectroscopy of $CO_2^{\bullet-}$ formation. **d)** Stern−Volmer luminescence quenching experiments. **e)** Time-course $^{1}B/^{19}F$ NMR study of $[BF_2(pin)]^-$ formation in the presence of HBpin.

Density functional theory (DFT) calculations were performed to further clarify the reaction mechanism and site-selectivity control (Fig. 6). The computational findings indicate that the fluorobenzyl radical **^{2}R1** initially adds to alkene via **^{2}TS-1** with an energy barrier of 18.1 kcal/mol, resulting in the formation of a stable alkyl radical intermediate **^{2}R2**. As documented in prior studies[45,46], this radical intermediate shows *β*-hydrogen atom transfer (*β*-HAT) reactivity in the presence of Co-TPP(II) (**[^{2}Co^{II}]**). The Gibbs free energy differences for the HAT processes at the Z/E configurations of the radical center were calculated to be 8.0 kcal/mol (via **^{OSS}TS-2**) and 13.1

kcal/mol (via ^{OSS}**TS-3**), respectively. Product **3bb** is formed via the cobaloxime(II)-assisted HAT transition state ^{OSS}**TS-2**. Subsequently, the exergonic proton transfer between the reactive **[^{1}Co^{III}]-H** and base, such as DIPEA, generates **[^{1}Co^{I}]** via ^{1}**TS-5**. This process is exergonic by 2.9 kcal/mol. Finally, through oxidation promoted by the ^{2}**Ir^{IV}** compound, the **[^{1}Co^{I}]** intermediate is converted back to the active **[^{2}Co^{II}]** catalyst, facilitating catalytic turnover, thus enabling catalyst regeneration. Moreover, there might be another adjacent position for the *β*-HAT process in the radical intermediate ^{2}**R2**. The Gibbs free energy barrier of ^{OSS}**TS-4** is 12.7 kcal/mol, which is 4.7 kcal/mol higher than that of ^{OSS}**TS-2**. The higher energy barrier can be attributed to the increased ligand-radical steric repulsion (See Figure S25 for details).

To further clarify the *E*/*Z*-selectivity of product and determine the influencing factors, the quantitative steric-electronic effects dissection (QSED) model developed in our group[50] is utilized to quantify the energies of steric effect (ΔE_{steric}), electronic effect (ΔE_{elec}), and dispersion interaction (ΔE_{disp}). The distortion-interaction analysis suggests that the difference in interaction energies ($\Delta\Delta E_{int}$ = 6.2 kcal/mol) is critical for the *E*/*Z*-selectivity. Subsequently, the detailed dissection results were illustrated in a pie chart (Figure 4b) to present a better visual representation. Because the electronic effect is decomposed into charge transfer (ΔE_{ct}), polarization (ΔE_{pol}), and electrostatics (ΔE_{elstat}), the pie chart consists of five sectors in total. Each sector represents the comparison of each energy term between ^{OSS}**TS-3** versus ^{OSS}**TS-2** ($\Delta\Delta E$). The positive value indicates that this term favors ^{OSS}**TS-2**, i.e. the *E*-selective HAT. According to the proportions of different sectors, the dispersion interaction is the dominant factor that promotes *E*-selective HAT transition state ^{OSS}**TS-2**. This quantitative dissection results account for the origin of *E*/*Z*-selectivity.

Based on the foregoing results, a plausible mechanism was proposed in Fig. 6c. Upon excitation, the Ir(III) complex initiates a SET to the polyfluoroalkyl compounds, yielding a radical anion alongside an Ir(IV) species. The resulting radical anion undergoes C–F bond fragmentation to generate a perfluoroalkyl radical and fluoride, with HBpin serving primarily as a fluoride scavenger that captures the liberated fluoride and suppresses back-electron transfer. The perfluoroalkyl radical then adds to the olefin in an anti-Markovnikov manner to form a carbon-centered radical, which is subsequently converted to the final product via a Co(II)-mediated selective hydrogen atom transfer (HAT) process that produces a Co(III)–H species. Deprotonation of the Co(III)–H intermediate regenerates the Co(I) complex[51], which in turn reduces the Ir(IV) species back to Ir(III) via a second SET, thereby completing the catalytic cycle.

Discussion

In conclusion, we have developed a photoredox/methylcobalamin-catalyzed radical defluoroallylation method for polyfluoroalkyl compounds. This method selectively cleaves C(sp^3)–F bonds under mild conditions, enabling site-selective allylic fluoroalkylation using readily available alkenes or natural terpenes. Mechanistic investigations reveal that the transformation proceeds through a HAT pathway mediated by methylcobalamin, which preferentially cleaves robust primary allylic C–H bonds. This precise reorganization of the olefin framework circumvents the formation of isomeric mixtures, thereby ensuring remarkable site control. Collectively, our findings establish a robust platform for the selective transformation of polyfluoroalkyl compounds and open new avenues for the streamlined assembly of complex fluorinated architectures.

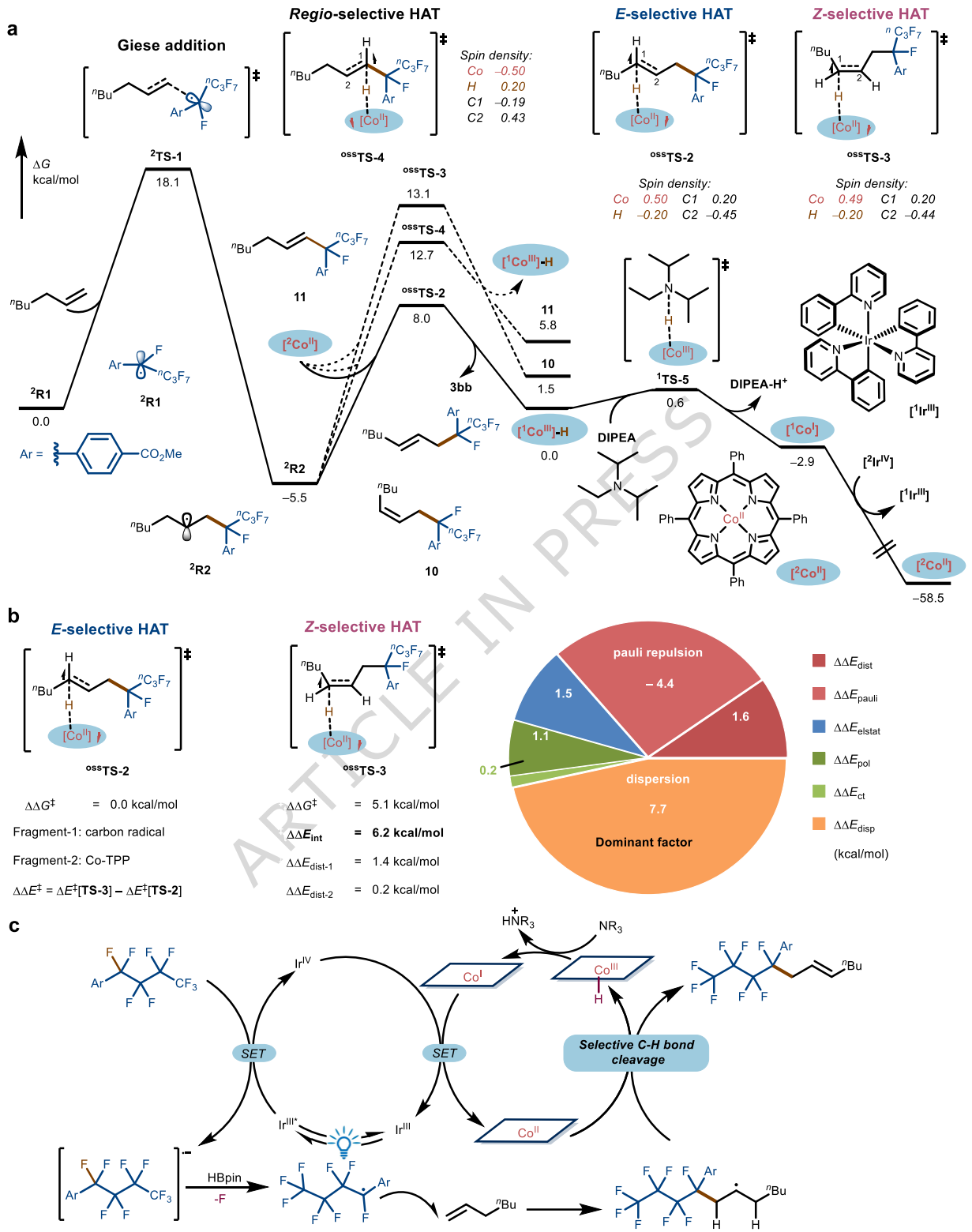

Fig. 6 | DFT calculations and proposed mechanism a) DFT study of **3bb** formation through the Giese addition of radical $\mathbf{R_f}$ and the Co-TPP (II)-assisted HAT process. Free energy profiles were calculated at the M06/6-311+G(d,p)-SDD/SMD(2-Ethoxyethanol, eps=13.38)//B3LYP-D3(BJ)/6-31G(d)-LANL2DZ level of theory. **b)** Quantitative steric-electronic effects dissection (QSED) of transition states **TS-2** and **TS-3** through the combination of distortion-interaction analysis and energy decomposition analysis (EDA). The EDA calculation was performed at M06-L/6-311+G(d,p)-SDD/SMD(2-Methoxyethanol) level of theory based on structures optimized using B3LYP-D3(BJ)/6-31G(d)-LANL2DZ. **c)** Proposed mechanism.

Methods:

General Information:

All reactions were conducted under an inert nitrogen atmosphere unless otherwise stated. Solvents were degassed prior to use. Photochemical reactions were irradiated using 3 W blue LEDs. After completion, solvents were removed under reduced pressure, and crude mixtures were purified by column chromatography on neutral alumina or silica gel as specified. TLC was used to monitor reaction progress. All commercially available reagents were used without further purification unless noted.

Synthesis of fluoroalkyl radical precursors:

Copper-mediated coupling procedure:

A solution of copper powder (11.3 mmol, 0.723 g), 2,2′-bipyridine (0.434 mmol, 0.0677 g) and aryl iodide (ArI, 5.15 mmol) in DMSO (8 mL) was prepared, and perfluoroalkyl iodide (6.12 mmol) was added. The reaction mixture was stirred at 80 °C for 48 h. After cooling to room temperature, the mixture was extracted with chloroform (10 mL × 3). The combined organic layers were washed with aqueous NH_3 (20 mL × 2) and brine (20 mL), dried over $MgSO_4$, filtered, and concentrated under reduced pressure. The crude residue was purified by column chromatography to afford the corresponding fluoroalkyl radical precursor.

Synthesis of trifluoroacetamide derivatives:

To a solution of aniline (5 mmol, 1 equiv.) and triethylamine (1.5 equiv.) in DCM (30 mL) at 0 °C, trifluoroacetic anhydride (1.2 equiv.) was added dropwise. The reaction mixture was allowed to warm to room temperature and stirred until TLC indicated full consumption of aniline. The solvent was removed under reduced pressure, and the resulting crude material was purified by flash chromatography on silica gel to give the desired trifluoroacetamide precursor.

Esterification procedure for preparing fluoroalkyl-containing precursors:

A solution of alcohol (10 mmol) and 4-(perfluorobutyl)benzoic acid (2.83 g, 10 mmol) in DCM (30 mL) was cooled to 0 °C. 1-(3-Dimethylaminopropyl)-3-ethylcarbodiimide hydrochloride (12 mmol) and DMAP (1.2 mmol) were added. The mixture was stirred at room temperature until TLC indicated complete consumption of the alcohol. The reaction was quenched with water and extracted with DCM (3 ×). The combined organic layers were washed with brine, dried over Na_2SO_4, filtered and evaporated. The residue was purified by flash chromatography (petroleum ether/ethyl acetate = 20:1) to afford the desired ester precursor.

Defluoroallylation of perfluoroalkylarenes with olefins:

A solution of perfluoroalkylarenes **1** (0.2 mmol), olefins (6 equiv.), *fac*-Ir(ppy)$_3$ (0.5 mol%), methylcobalamin (3 mol%), HBpin (0.3 equiv.), *N*, *N*-diisopropylethylamine (0.25 equiv.) in degassed 2-ethoxyethanol (6.0 mL) were stirred under nitrogen atmosphere and irradiated by 3W blue LEDs for 36 h. After completion of the reaction, the solv ent was removed under reduced pressure by rotary evaporation, and then purified by column chromatography on neutral alumina.

Defluoroallylation of perfluoroalkylarenes with terpenes:

A solution of perfluoroalkylarenes **1** (0.2 mmol), olefins (6 equiv.), *fac*-Ir(ppy)$_3$ (1 mol%), methylcobalamin (3 mol%), NaOAc (0.5 equiv.), LiF (0.5 equiv.), *N*, *N*-diisopropylethylamine (0.5 equiv.) in degassed 2-ethoxyethanol (6.0 mL) were stirred under nitrogen atmosphere and irradiated by 3W blue LEDs for 36 h. After completion of the reaction, the solvent was removed under reduced pressure by rotary evaporation. Then purified by column chromatography on neutral alumina.

Defluoroallylation of perfluoroalkylarenes with monosubstituted olefins:

A solution of perfluoroalkylarenes **1** (0.2 mmol), olefins (6 equiv.), *fac*-Ir(ppy)$_3$ (1 mol%), Co-TPP (3 mol%), HBpin (0.3 equiv.), *N*, *N*-diisopropylethylamine (0.25 equiv.) in degassed 2-

ethoxyethanol (6.0 mL) were stirred under nitrogen atmosphere and irradiated by 3W blue LEDs for 48 h. After completion of the reaction, the solvent was removed under reduced pressure by rotary evaporation, and then purified by column chromatography on neutral alumina.

Defluoroallylation of polyfluorinated aliphatic amides with olefins:

A solution of perfluoroalkyl reagent **1**, olefin **2** (6.0 equiv.), *fac*-Ir(ppy)$_3$ (3 mol%, 3.9 mg), methylcobalamin (3 mol%, 8.0 mg), HBpin (30.7 mg, 1.2 equiv.), *N*,*N*-diisopropylethylamine (77.4 mg, 3 equiv.), and Cs_2CO_3 (65.2 mg, 1 equiv.) in degassed DMF (6.0 mL) was stirred under CO_2 atmosphere (headspace volume: 14 mL) and irradiated by 3W blue LEDs for 36 h. After completion of the reaction, the reaction mixture was extracted with ethyl acetate (15 mL × 3). The combined organic layers were washed with saturated brine (20 mL), then dried over anhydrous Na_2SO_4. The solvent was removed under reduced pressure using rotary evaporation. The crude product was then purified by column chromatography on neutral alumina.

Data Availability:

All data supporting the findings of this study are included in the article, its Supplementary Information and the accompanying Source Data file. The Supplementary Information contains experimental details, characterization data, copies of NMR spectra for all new compounds, and additional density functional theory (DFT) calculation data. The Source Data file provides the Cartesian coordinates of all DFT-optimized structures. Source data are provided with this paper. All data are available from the corresponding author upon request.

References

1 Buck, R. C., Murphy, P. M., & Pabon, M. Chemistry, Properties, and Use of Commercial Fluorinated Surfactants. In *The Handbook of Environmental Chemistry Polyfluorinated Chemicals and Transformation Products* (ed. T. P. Knepper & F. T. Lange), Springer Berlin Heidelberg, **17**, 1–24, (2012). DOI: 10.1007/978-3-642-21872-9.

2 Scheringer, M. *et al.* An overview of the uses of per- and polyfluoroalkyl substances (PFAS). *Environ. Sci.: Processes Impacts*, **22**, 2345-2373, (2020). DOI: 10.1039/d0em00291g

3 Zhou, M., & Foudazi, R. Towards a universal model for the foaming behavior of surfactants: a case study on per- and polyfluoroalkyl substances (PFAS). *Soft Matter*, **20**, 9343–9359, (2024). DOI: 10.1039/d4sm00931b.

4 Trang, B. *et al.* Low-temperature mineralization of perfluorocarboxylic acids. *Science*, **377**, 839–845, (2022). DOI: 10.1126/science.abm8868.

5 Amii, H., & Uneyama, K. C−F Bond Activation in Organic Synthesis. *Chem. Rev.*, **109**, 2119–2183, (2009). DOI: 10.1021/cr800388c.

6 Bentel, M. J., Yu, Y., Xu, L., Li, Z., Wong, B. M., Men, Y., & Liu, J. Defluorination of per- and polyfluoroalkyl substances (PFASs) with hydrated electrons: Structural dependence and implications to PFAS remediation and management. *Environ. Sci. Technol.*, **53**, 3718–3728, (2019). DOI: 10.1021/acs.est.8b06648.

7 Liu, J., Van Hoomissen, D. J., Liu, T., Maizel, A., Huo, X., Fernández, S. R., Ren, C., Xiao, X., Fang, Y., Schaefer, C. E., Higgins, C. P., Vyas, S., & Strathmann, T. J. Reductive defluorination of branched per- and polyfluoroalkyl substances with cobalt complex catalysts. *Environ. Sci. Technol. Lett.*, **5**, 289–294, (2018). DOI: 10.1021/acs.estlett.8b00122.

8 Nishimoto, Y., Sugihara, N., & Yasuda, M. C(sp^3)–F bond transformation of perfluoroalkyl compounds mediated by visible-light photocatalysis: Spin-center shifts and radical/polar crossover processes via anionic intermediates. *Synthesis*, **54**, 2765–2777, (2022). DOI: 10.1055/a-1755-3476.

9 Liu, J.-W., Li, S.-Y., Xu, J., & Xu, H.-J. Recent advance in the C−F bond functionalization of trifluoromethyl aromatic and carbonyl compounds. *ChemCatChem*, **16**, e202301504, (2024). DOI: 10.1002/cctc.202301504.

10 Luo, Y.-C., Tong, F.-F., Zhang, Y., He, C.-Y., & Zhang, X. Visible-light-induced palladium-catalyzed selective defluoroarylation of trifluoromethylarenes with arylboronic acids. *J. Am. Chem. Soc.*, **143**, 13971–13979, (2021). DOI: 10.1021/jacs.1c07459.

11 Luo, C., & Bandar, J. S. Selective defluoroallylation of trifluoromethylarenes. *J. Am. Chem. Soc.*, **141**, 14120–14125, (2019). DOI: 10.1021/jacs.9b07766.

12 Liu, C., Shen, N., & Shang, R. Photocatalytic defluoroalkylation and hydrodefluorination of trifluoromethyls using o-phosphinophenolate. *Nat. Commun.*, **13**, 354, (2022). DOI: 10.1038/s41467-022-28007-2.

13 Chen, M., Cui, Y., Chen, X., Shang, R., & Zhang, X. C−F bond activation enables synthesis of aryl difluoromethyl bicyclopentanes as benzophenone-type bioisosteres. *Nat. Commun.*, **15**, 419, (2024). DOI: 10.1038/s41467-023-44653-6.

14 Douvris, C., & Ozerov, O. V. Hydrodefluorination of perfluoroalkyl groups using silylium-carborane catalysts. *Science*, **321**, 1188–1190, (2008). DOI: 10.1126/science.1159979.

15 Yoshida, S., Shimomori, K., Kim, Y., & Hosoya, T. Single C−F bond cleavage of trifluoromethylarenes with an ortho-silyl group. *Angew. Chem. Int. Ed.*, **55**, 10406–10409, (2016). DOI: 10.1002/anie.201604776.

16 Mandal, D., Gupta, R., Jaiswal, A. K., & Young, R. D. Frustrated Lewis pair mediated selective single fluoride substitution in trifluoromethyl groups. *J. Am. Chem. Soc.*, **142**, 2572–2578, (2020). DOI: 10.1021/jacs.9b12167.

17 Yu, Y.-J. *et al.* Sequential C–F bond functionalizations of trifluoroacetamides and acetates via spin-center shifts. *Science*, **371**, 1232–1240, (2021). DOI: 10.1126/science.abg0781.

18 Chen, K., Berg, N., Gschwind, R., & König, B. Selective single C(sp3)−F bond cleavage in trifluoromethylarenes: Merging visible-light catalysis with Lewis acid activation. *J. Am. Chem. Soc.*, **139**, 18444–18447, (2017). DOI: 10.1021/jacs.7b10755.

19 Wang, H., & Jui, N. T. Catalytic defluoroalkylation of trifluoromethylaromatics with unactivated alkenes. *J. Am. Chem. Soc.*, **140**, 163–166, (2018). DOI: 10.1021/jacs.7b12590.

20 Vogt, D. B., Seath, C. P., Wang, H., & Jui, N. T. Selective C–F functionalization of unactivated trifluoromethylarenes. *J. Am. Chem. Soc.*, **141**, 13203–13211, (2019). DOI: 10.1021/jacs.9b06004.

21 Sap, J. B. I. *et al.* Organophotoredox hydrodefluorination of trifluoromethylarenes with translational applicability to drug discovery. *J. Am. Chem. Soc.*, **142**, 9181–9187, (2020). DOI: 10.1021/jacs.0c03881.

22 Wang, J. *et al.* Late-stage modification of drugs via alkene formal insertion into benzylic C−F bond. *Angew. Chem. Int. Ed.*, **62**, e202215062, (2023). DOI: 10.1002/anie.202215062.

23 Campbell, M. W. *et al.* Photochemical C–F activation enables defluorinative alkylation of trifluoroacetates and -acetamides. *J. Am. Chem. Soc.*, **143**, 19648–19654, (2021). DOI: 10.1021/jacs.1c11059.

24 Ye, J.-H., Bellotti, P., Heusel, C., & Glorius, F. Photoredox-catalyzed defluorinative functionalizations of polyfluorinated aliphatic amides and esters. *Angew. Chem. Int. Ed.*, **61**, e202115456, (2022). DOI: 10.1002/anie.202115456.

25 Yamauchi, Y., Sakai, K., Fukuhara, T., Hara, S., & Senboku, H. Synthesis of 2-aryl-2,3,3,3-tetrafluoropropanoic acids, tetrafluorinated fenoprofen and ketoprofen by electrochemical carboxylation of pentafluoroethylarenes. *Synthesis*, **20**, 3375–3377, (2009). DOI: 10.1055/s-0029-1216993.

26 Utsumi, S., Katagiri, T., & Uneyama, K. Cu-deposits on Mg metal surfaces promote electron transfer reactions. *Tetrahedron*, **68**, 1085–1091, (2012). DOI: 10.1016/j.tet.2011.11.082.

27 Ichitsuka, T., Fujita, T., Arita, T., & Ichikawa, J. Double C–F bond activation through *β*-fluorine elimination: Nickel-mediated [3+2] cycloaddition of 2-trifluoromethyl-1-alkenes with alkynes. *Angew. Chem., Int. Ed.*, **53**, 7564–7568, (2014). DOI: 10.1002/anie.201402695.

28 Sugihara, N., Suzuki, K., Nishimoto, Y., & Yasuda, M. Photoredox-catalyzed C–F bond allylation of perfluoroalkylarenes at the benzylic position. *J. Am. Chem. Soc.*, **143**, 9308–9313, (2021). DOI: 10.1021/jacs.1c03760.

29 Sugihara, N., Nishimoto, Y., Osakada, Y., Fujitsuka, M., Abe, M., & Yasuda, M. Sequential C–F bond transformation of the difluoromethylene unit in perfluoroalkyl groups: A combination of fine-tuned phenothiazine photoredox catalyst and Lewis acid. *Angew. Chem. Int. Ed.*, **63**, e202401117, (2024). DOI: 10.1002/anie.202401117.

30 Chandra, A. K., & Uchimaru, T. A DFT study on the C−H bond dissociation enthalpies of haloalkanes: Correlation between the bond dissociation enthalpies and activation energies for hydrogen abstraction. *J. Phys. Chem. A*, **104**, 9244–9249, (2000). DOI: 10.1021/jp001815x.

31 Bott, G., Field, L. D., & Sternhell, S. Steric effects: A study of a rationally designed system. *J. Am. Chem. Soc.*, **102**, 5618–5626, (1980). DOI: 10.1021/ja00537a036.

32 Schlosser, M., & Michel, D. About the "physiological size" of fluorine substituents: Comparison of sensorially active compounds with fluorine and methyl substituted analogues. *Tetrahedron*, **52**, 99–108, (1996). DOI: 10.1016/0040-4020(95)00886-d.

33 Romero, N. A., & Nicewicz, D. A. Organic photoredox catalysis. *Chem. Rev.*, **116**, 10075–10166, (2016). DOI: 10.1021/acs.chemrev.6b00057.

34 Zhao, H., & Leonori, D. Minimization of back-electron transfer enables the elusive sp3 C−H functionalization of secondary anilines. *Angew. Chem. Int. Ed.*, **60**, 7669–7674, (2021). DOI: 10.1002/anie.202100051.

35 Tang, S., Liu, K., Liu, C., & Lei, A. Olefinic C–H functionalization through radical alkenylation. *Chem. Soc. Rev.*, **44**, 1070–1082, (2015). DOI: 10.1039/c4cs00347k.

36 Wu, Z. *et al.* Multi-site programmable functionalization of alkenes via controllable alkene isomerization. *Nat. Chem.*, **15**, 988–997, (2023). DOI: 10.1038/s41557-023-01209-x.

37 Huang, H.-M., Bellotti, P., & Glorius, F. Transition metal-catalysed allylic functionalization reactions involving radicals. *Chem. Soc. Rev.*, **49**, 6186–6197, (2020). DOI: 10.1039/d0cs00262c.

38 Li, J. *et al.* Site-specific allylic C–H bond functionalization with a copper-bound *N*-centred radical. *Nature*, **574**, 516–521, (2019). DOI: 10.1038/s41586-019-1655-8.

39 Tanabe, S., Mitsunuma, H., & Kanai, M. Catalytic allylation of aldehydes using unactivated alkenes. *J. Am. Chem. Soc.*, **142**, 12374–12381, (2020). DOI: 10.1021/jacs.0c04735.

40 Ding, Y., Wu, J., Zhang, T., Liu, H., & Huang, H. Site-selective carbonylative cyclization with two allylic C–H bonds enabled by radical differentiation. *J. Am. Chem. Soc.*, **146**, 19635–19642, (2024). DOI: 10.1021/jacs.4c05360.

41 Zhou, F.-Y., & Jiao, L. Asymmetric defluoroallylation of 4-trifluoromethylpyridines enabled by umpolung C−F bond activation. *Angew. Chem. Int. Ed.*, **61**, e202201102, (2022). DOI: 10.1002/anie.202201102.

42 Skubi, K. L., Blum, T. R., & Yoon, T. P. Dual catalysis strategies in photochemical synthesis. *Chem. Rev.*, 116, 10035–10074, (2016). DOI: 10.1021/acs.chemrev.6b00018.

43 Fuchibe, K., Hatta, H., Oh, K., Oki, R., & Ichikawa, J. Lewis acid promoted single C–F bond activation of the CF_3 group: SN1′-type 3,3-difluoroallylation of arenes with 2-trifluoromethyl-1-alkenes. *Angew. Chem. Int. Ed.*, **56**, 5890–5893, (2017). DOI: 10.1002/anie.201701985.

44 Wang, S. *et al.* Cobalt-catalysed allylic fluoroalkylation of terpenes. *Nat. Synth.*, 2, 1202–1210, (2023). DOI: 10.1038/s44160-023-00365-9.
45 Wang, S. *et al.* Site-selective amination towards tertiary aliphatic allylamines. *Nat. Catal.*, **5**, 642–651, (2022). DOI: 10.1038/s41929-022-00818-y.
46 Wang, S. *et al.* Radical-triggered translocation of C–C double bond and functional group. *Nat. Chem.*, 16, 1621–1629, (2024). DOI: 10.1038/s41557-024-01633-7.
47 Song, L., Wang, W., Yue, J.-P., Jiang, Y.-X., Wei, M.-K., Zhang, H.-P., Yan, S.-S., Liao, L.-L., & Yu, D.-G. Visible-light photocatalytic di- and hydro-carboxylation of unactivated alkenes with CO_2. *Nat. Catal.*, **5**, 832–838, (2022). DOI: 10.1038/s41929-022-00841-z.
48 Hamdaoui, M., Liu, F., Cornaton, Y., Lu, X., Shi, X., Zhang, H., Liu, J., Spingler, B., Djukic, J.-P., & Duttwyler, S. An iridium-stabilized borenium intermediate. *J. Am. Chem. Soc.*, **144**, 18359–18374, (2022). DOI: 10.1021/jacs.2c06298.
49 Kuehn, L., Stang, M., Würtemberger-Pietsch, S., Friedrich, A., Schneider, H., Radius, U., & Marder, T. B. FBpin and its adducts and their role in catalytic borylations. *Faraday Discuss.*, **220**, 350–363, (2019). DOI: 10.1039/c9fd00053d.
50 Zheng, W.-F., Chen, J., Qi, X., & Huang, Z. Modular and diverse synthesis of amino acids via asymmetric decarboxylative protonation of aminomalonic acids. *Nat. Chem.*, 15, 1672–1682 (2023). DOI: 10.1038/s41557-023-01362-3.
51 Dam, P., Zuo, K., Azofra, L. M., & El-Sepelgy, O. Biomimetic photoexcited cobaloxime catalysis in organic synthesis. *Angew. Chem. Int. Ed.*, **63**, e202405775, (2024). DOI: 10.1002/anie.202405775.

Acknowledgments:

This work was supported by National Natural Science Foundation of China No. 22522112 (H.Y.) and No.22201222(X.Q.), the National Key R&D Program of China No. 2021YFA1500104 (A.L.) and NO. 2022YFA1505100 (H.Y.), Hubei Technological Innovation Program Funding 2025BAB025 (H.Y.), and the supercomputing system in the Supercomputing Center of Wuhan University (X.Q.). We thank Dr. Xue Zhou from the Core Research Facilities of CCMS (WHU) for her assistance with NMR analysis. We thank the support of the Opening Foundation of Xi'an Modern Chemistry Research Institute (grant number 204-J-2023-2325).

Author Contributions Statement:

H.Y. and D.R. conceived the work. D.R., H.Y., J.Y., B.W. and A.L. designed the experiments and analyzed the data. D.R., Y.W., and W.D. performed the synthetic experiments. S.W., J.Y., and P.W. contributed to EPR data. S.D. and X.Q. contributed to the DFT calculation. D.R. wrote original manuscript which revised by all authors.

Competing Interests Statement:

The authors declare no competing interests.

Editor's Summary

Selective functionalization of polyfluoroalkyl compounds is vital for advancing pharmaceuticals, agrochemicals, and high-performance materials but is hindered by the stability of C(sp^3)–F bonds. Here, the authors report a dual photoredox/cobalt catalytic strategy enabling redox-driven defluoroallylation of perfluoroalkylarenes and polyfluorinated aliphatic amides.

Peer review information: *Nature Communications* thanks the anonymous reviewer(s) for their contribution to the peer review of this work. A peer review file is available.